CeGaT GmbH | Paul-Ehrlich-Str. 23 | D-72076 Tübingen | Germany

Dr. Physician
University hospital of capital
Physician street 1
1234 capital
Country

Name	Doe
Forename	Jane
Date of birth	01.01.1901
Sex	female
Patient-ID	12345
Sample receipt	DD.MM.YYYY (EDTA blood) DD.MM.YYYY (Tumor-FFPE)
Your ID	8765432
Report date	DD.MM.YYYY

cc. encrypted via email to Dr. physician, physician@clinic.com

Report of somatic tumor mutations – Doe, Jane | 01.01.1901

Indication

Metastatic colorectal adenocarcinoma
Initial diagnosis 11/2016; pT4a N2a R0
Previous molecular tumor diagnostics: *KRAS* G12 wildtype

Material

Tumor tissue: Liver metastasis of a colorectal tumor
Sample extraction 12/2016, University Hospital of Capital
DNA-Isolation from FFPE material (16-123456-23) with estimated tumor content of 70% after macrodissection (Praxis für Humangenetik, Tübingen)

Normal tissue: EDTA blood

Order

Somatic molecular genetic analysis of a tumor-tissue sample:
Tumor panel-analysis TUM01, evaluation of somatic variants of potential clinical relevance
Test for microsatellite instability

SOMATIC VARIANTS WITH POTENTIAL CLINICAL RELEVANCE

We detected variants with potential therapeutic relevance in the current sample.

The results of this report should be evaluated against this patient's current clinical status and should be reviewed by an interdisciplinary tumor board.

Mutational load: high

We extrapolated a high mutational load of approximately 136.9 variants per megabase of DNA likely to be present within the exome of this tumor sample.

Copy number alterations: intermediate

Microsatellite instability: MSI (instable)

Analysis of five mononucleotide marker loci revealed high microsatellite instability.

Variants with potential therapeutic relevance:

Gene	Functional category	Variant	Transcript-ID	NAF	Potential therapeutic relevance
MSH6 (germline)	stop_gained	c.3132C>A; p.Tyr1044*	NM_000179.2	het.	Immune checkpoint therapy
NRAS	missense	c.35G>A; p.Gly12Asp	NM_002524.4	0.32	MEK inhibitors, resistance against EGFR-targeted antibody therapies, clinical trials
RB1	stop_gained	c.1396G>T; p.Glu466* and loss of wildtype-allele	NM_000321.2	0.37	Probably resistance to CDK4/6 inhibitors, clinical trials
TP53	essential_splice_site	c.672+1G>T; p.? and loss of wildtype-allele	NM_000546.5	0.33	Clinical trials
SMAD4	missense	c.1157G>A; p.Gly386Asp and loss of wildtype-allele	NM_005359.5	0.27	Probably resistance to gemcitabine, cetuximab and oxaliplatin

NAF: *Novel allele frequency*, the frequency with which the mutated allele was detected in the sequencing data (1 is 100%). The observed frequencies are influenced by the tumor content and do not correlate directly with the variant frequency in the tumor. **Het.:** heterozygous

RESULTS:

Mutational load:

We calculated 136.9 somatic variants per megabase of DNA to be present within the exome of this tumor sample. The mutational load of this tumor sample can be considered high (Chalmers et al., 2017, PMID: 28420421; Johnson et al., 2016, PMID: 27671167). The mutational load of this tumor sample (red bar) is depicted in the supplement information in relation to the mutational load published for different tumor entities.

Microsatellite instability:

Molecular pathology of the tumor specimen revealed in detail for five mononucleotide marker loci:

BAT25:	instable	NR22:	instable
BAT26:	stable	NR27:	instable
NR21:	stable		

The observed instability pattern at two or more markers indicates microsatellite instability, corresponding to a MSI-High status.

Copy number alterations:

Our sequencing data do provide evidence for the presence of copy number alteration (deletions and/or amplifications) of large genomic segments. These are listed in the following table.

Chromosomal region	Functional category	Variant	Copy number	Affected genes with potential therapeutic relevance
chr3	heterozygous deletion	p-arm, partial	1	*MLH1, BAP1, PBRM1*
chr4	heterozygous deletion		1	-
chr6	heterozygous deletion	q-arm, partial	1	*ARID1B*
chr13q	heterozygous deletion	q-arm	1	*BRCA2, RB1*
chr16p	loss of heterozygosity	p-arm	2	*PALB2*
chr16q	heterozygous deletion	q-arm	1	*CDH1*
chr17p	heterozygous deletion	p-arm	1	*TP53*
chr17q	duplication	q-arm	3	*ERBB2*
chr18q	heterozygous deletion	q-arm	1	*CDH2, SMAD4, DCC*

The sensitivity of copy number detection depends on the sample's tumor content and the sample's overall quality. Copy numbers as well as breakpoints are estimated on the basis of the NGS data and should be treated as estimated values. The set of candidate genes represents a selection only and makes no claim of completeness. Please be aware that copy number variants likely cover a large number of genes. Possible interactions between these genes may impair reliable prediction of single gene effects on the analyzed tumor.

However, please note that next generation sequencing is not the gold standard for detection of copy number variation. **If a precision medicine approach targeting the detected copy number alterations is going to be considered for further treatment, these findings should be validated by a second method (e.g. FISH, IHC).**

Germline variants with potential clinical relevance:

The detected variant c.3132C>A; p.Tyr1044* in gene *MSH6* is a germline mutation. A medical report on hereditary diseases can be arranged on the basis of genetic counseling.

High mutational load and MSI; germline mutation *MSH6*, c.3132C>A; p.Tyr1044*, NM_000179.2

We have calculated a value of approximately 136.9 somatic variants per megabase of DNA to be present within the exome of this tumor sample. Tumors possessing a high mutational load are expected to be sensitive to immune therapy, since they are likely to be expressing a large number of neo-antigens. The use of drugs targeting immune checkpoint inhibitors, such as anti-PD-1/PD-L1 and anti-CTLA-4, support the tumor specific immune response and have been shown to successfully target different tumor entities with high mutational load (Johnson et al., 2016, PMID: 27671167; Rizvi et al., 2015, PMID: 25765070; Snyder et al., 2014, PMID:25409260; Le et al., 2015, PMID: 26028255; Bouffet et al., 2016, PMID:27001570). Immune checkpoint inhibitors are approved drugs for the treatment of melanoma, lung cancer, kidney cancer, Hodkin's lymphoma, urothelial carcinoma and head and neck cancer. In cases with high mutational load, a broad applicability of immune checkpoint inhibitors is generally assumed for different tumor entities (Colli et al., 2016 and 2017, PMID: 27197178, PMID: 28446466).

The detected heterozygous truncating mutation in *MSH6* is present in the tumor as well as in the blood sample of your patient. The MSH6 protein plays an important role in DNA mismatch repair. Especially patients with mismatch repair-deficient colorectal cancer, that accumulate a high number of somatic mutations, were shown to benefit from anti-PD-1 immune checkpoint therapy in a phase II study using Pembrolizumab (Le et al., 2015, PMID: 26028255). Alongside with somatic microsatellite instability this variant in gene *MSH6* is consistent with the determined MSI status. Therapeutically, this condition is associated with a poor response to 5-fluorouracil (Ribic et al., 2003, PMID: 12867608), whereas patients could benefit from treatment with immune checkpoint inhibitors (Passardi et al., 2017, PMID: 28635639).

Possible therapeutic strategies for patients with highly mutated and MSI colorectal cancer are listed in the supplementary information.

NRAS, c.35G>A; p.Gly12Asp, NM_002524.4:

NRAS encodes N-Ras, a member of the Ras family proteins, which are membrane-associated small GTPases that mediate transduction of growth signals.

NRAS-p.Gly12Asp is an activating mutation. Activating RAS mutations, including those in *NRAS*, result in activation of downstream pathways, including the Raf/MEK/ERK pathway (Pylayeva-Gupta et al., 2011, PMID: 21993244). *NRAS* mutations have been found to be mutually exclusive with *KRAS* and *BRAF* mutations in colorectal carcinoma (Pentheroudakis et al., 2013, PMID: 23374602; Vaughn et al., 2011, PMID: 21305640; Janku et al., 2013, PMID: 23400451; De Roock et al., 2010, PMID: 20619739; Irahara et al., 2010, PMID: 20736745; Netzel and Grebe, 2013, PMID: 23832066; Smith et al., 2013, PMID: 23741067). Most activating mutations in exon 2, 3 or 4 of the *NRAS* or *KRAS* gene are associated with an resistance against EGFR-targeted antibody therapies (De Roock et al., 2010, PMID: 20619739; Hsu et al., 2016; PMID: 26989027; Schirippa et al., 2015, PMID: 24806288; Morris et al., 2014; Van Cutsem et al., 2016, PMID: 27380959).

Some MEK inhibitors such as trametinib and cobimetinib have been approved by the FDA to treat melanoma. Trametinib and other MEK inhibitors, alone or in combination therapy, are in clinical trials, as are multiple other approaches targeting N-Ras signaling (Flaherty et al., 2012, PMID: 22663011; Jänne et al., 2013, PMID: 23200175; Britten, 2013, PMID: 23443307).

Possible therapeutic strategies for patients with *NRAS*-mutated colorectal cancer are listed in the supplementary information.

CeGaT GmbH | Paul-Ehrlich-Str. 23 | D-72076 Tübingen | Germany
Tel: + 49 7071 565 44 55 | Fax: + 49 7071 565 44 56 | info@cegat.de | www.cegat.de
Court District Stuttgart - HRB 729958 | VAT No: DE265504070
VR Bank Tübingen eG | IBAN: DE20 6406 1854 0021 2890 00 | SWIFT / BIC: GENODES1STW
Managing Directors: Dr. Dr. Saskia Biskup, Dr. Dirk Biskup

RB1, c.1396G>T; p.Glu466*; NM_000321.2:

RB1 encodes the retinoblastoma protein (Rb), a tumor suppressor and negative regulator of the cell cycle. Loss of Rb function, which has been identified in many cancer types due to various mechanisms, results in the upregulation of transcription and cell proliferation (Burkhart and Sage, 2008, PMID: 18650841; Knudsen and Knudsen, 2008, PMID: 19143056).

The detected variant c.1396G>T; p.Glu466* in *RB1* most likely leads to a shorter, inactive protein. In addition, the wildtype allele is lost by heterozygous deletion of the chromosome 13q.

Loss of *RB1* has been associated with a lack of response to CDK4/6 inhibitors (Indovina et al., 2015, PMID: 26160835; Fry et al., 2004, PMID: 15542782; Michaud et al., 2010, PMID: 20354191). At this time, there are no therapeutic options to target the inactivation of Rb. Preclinical studies are actively investigating possible therapies to address Rb inactivation, exploring aurora kinase inhibitors, Bcl-2 family inhibitors, and Notch pathway activation (Hook et al., 2012, PMID: 22222631, Allaman-Pillet et al., 2013, PMID: 21955141, Viatour et al., 2011, PMID: 21875955, Knudsen und Wang, 2010, PMID: 20145169).

As possible therapeutic strategies targeting *RB1* are currently of low evidence, we renounced to list therapies.

TP53, c.672+1G>T; p.?; NM_000546.5:

TP53 is a tumor suppressor. Alterations in *TP53* may result in a loss of p53 function, yet an increase in the expression and stability of the mutant p53 protein in the nucleus, sometimes leading to oncogenic effects including genomic instability and excessive cell proliferation (Levine, 1997, PMID: 9039259; Wang et al., 2005, PMID: 15625370; Koga et al., 2001, PMID: 11400116; Kato et al., 2003, PMID: 12826609; Houben et al., 2011, PMID: 21760960; Olivier et al., 2009, PMID: 18802452).

The *TP53*-c.672+1G>T; p.? variant is located in an essential splice site and probably results in a splicing change. This variant was first described as germline variant in Li-Fraumeni/Li-Fraumeni-like syndromes (Achatz et al., 2007, PMID: 16494995). In addition, the wildtype allele is lost by heterozygous deletion of the chromosome 17p.

At present, there are no approved therapies targeting *TP53* alterations, despite their high prevalence in cancer. Therapeutic approaches under investigation include gene therapy for *TP53* and (dendritic cell-based) *TP53* vaccines (Schuler et al., 2014, PMID: 24583792; Vermeij et al., 2011, PMID: 21541192; Saito et al., 2014, PMID: 24982341). Additional p53-targeted approaches under clinical investigation, which may be relevant in the context of certain *TP53* alterations, include kevetrin and ALT-801 (Kumar et al., 2012, AACR 2012, Abstract 2874; Fishman et al., 2011, PMID: 21994418). ALT-801 is restricted to HLA-A*02:01 positive patients. Tumors with *TP53* mutations may be sensitive to the Wee1 inhibitor MK-1775, and clinical trials are currently underway for patients with solid tumors (Hirai et al., 2010, PMID: 20107315; Bridges et al., 2011, PMID: 21799033). Inhibition of Aurora kinase A, a controller of chromatin segregation, is another therapeutic approach under investigation for *TP53*-mutated cancers (Vilgelm et al., 2015, PMID: 25398437; Li et al., 2015, PMID: 25512615; Katayama and Sen, 2011, PMID: 21761334; Tentler et al., 2015, PMID: 25758253; Kalous et al., 2013, PMID: 24091768).

Possible therapeutic strategies for patients with *TP53* mutated tumors are listed in the supplementary information.

SMAD4, c.1157G>A; p.Gly386Asp; NM_005359.5:

SMAD4 is a tumor suppressor gene, which encodes for a transcription factor of the TGF-β-signaling. Inactivating mutations in *SMAD4* or reduced expression of *SMAD4* are often associated with an activation of *KRAS* (Bardeesy et al., 2006, PMID: 17114584).

The detected variant c.1157G>A; p.Gly386Asp in *SMAD4* is most likely an inactivating mutation, which results in decreased transcriptional activity on Smad4 (Gallione et al., 2010, PMID: 20101697; Yoshioka et al., 2015, PMID: 26488212). In addition, the q-arm of chromosome 18 depicts a heterozygous deletion of the wildtype allele.

A clincial study showed, that patients with low *SMAD4* expression do not profit from treatment with cetuximab, gemcitabine and oxaliplatin (Crane et al., 2011, PMID: 21709185). Preclinical studies showed that loss of *SMAD4* in pancreatic carcinomas leads to resistance to gemcitabine, but to sensitivity to cisplatin (Cui et al., 2012, PMID: 22753594).

Please do not hesitate to contact us if you have any questions.

With kind regards,

Dr. med. Dr. rer. nat. Saskia Biskup Consultant for Human Genetics	Dr. rer. nat. Diagnostic 3 Diagnostics	Dr. rer. nat. Diagnostic 2 Diagnostics	Dr. rer. nat. Diagnostic 1 Diagnostics

ADDITIONAL INFORMATION:

Investigated genes

Somatic tumor panel (TUM01) contains interpretation of the following cancer-relevant genes:

ABL1, *ABL2*, *ACD*, *AIP*, *AJUBA*, *AKT1*, *AKT2*, *AKT3*, *ALK*, *AMER1*, *ANKRD26*, *APC*, *AR*, *ARAF*, *ARHGAP35*, *ARID1A*, *ARID1B*, *ARID2*, *ARID5B*, *ASXL1*, *ASXL2*, *ATG2B*, *ATM*, *ATP1A1*, *ATR*, *ATRX*, *AURKA*, *AURKB*, *AURKC*, *AXIN1*, *AXIN2*, *AXL*, *B2M*, *BAP1*, *BARD1*, *BCL10*, *BCL11A*, *BCL11B*, *BCL2*, *BCL3*, *BCL6*, *BCL9*, *BCOR*, *BCORL1*, *BCR*, *BIRC2*, *BIRC3*, *BIRC5*, *BLM*, *BMPR1A*, *BRAF*, *BRCA1*, *BRCA2*, *BRD3*, *BRD4*, *BRIP1*, *BTK*, *BTNL2*, *BUB1B*, *C11ORF30*, *CALR*, *CAMK2G*, *CARD11*, *CASP8*, *CBFB*, *CBL*, *CBLB*, *CBLC*, *CCDC6*, *CCND1*, *CCND2*, *CCND3*, *CCNE1*, *CD274*, *CD38*, *CD52*, *CD58*, *CD79A*, *CD79B*, *CD82*, *CDC73*, *CDH1*, *CDH11*, *CDH2*, *CDK12*, *CDK4*, *CDK6*, *CDK8*, *CDKN1A*, *CDKN1B*, *CDKN1C*, *CDKN2A*, *CDKN2B*, *CDKN2C*, *CEBPA*, *CEP57*, *CHD1*, *CHD2*, *CHD4*, *CHEK1*, *CHEK2*, *CIC*, *CIITA*, *CKS1B*, *CNOT3*, *COL1A1*, *COMMD1*, *CREB1*, *CREBBP*, *CRKL*, *CRTC1*, *CRTC2*, *CSF1R*, *CSF2*, *CSF3R*, *CSMD1*, *CSNK1A1*, *CTCF*, *CTLA4*, *CTNNA1*, *CTNNB1*, *CUL4B*, *CUX1*, *CXCR4*, *CYLD*, *CYP2A7*, *DAXX*, *DCC*, *DDB2*, *DDR1*, *DDR2*, *DDX11*, *DDX3X*, *DDX41*, *DEK*, *DHFR*, *DICER1*, *DIS3*, *DIS3L2*, *DKC1*, *DNMT1*, *DNMT3A*, *DOT1L*, *DPYD*, *EBP*, *EGFR*, *EGLN1*, *EGR2*, *EGR3*, *ELAC2*, *ELANE*, *ELF3*, *EML4*, *EP300*, *EPAS1*, *EPCAM*, *EPHA2*, *EPHA3*, *EPHA4*, *EPHB4*, *EPHB6*, *ERBB2*, *ERBB3*, *ERBB4*, *ERCC1*, *ERCC2*, *ERCC3*, *ERCC4*, *ERCC5*, *ERG*, *ERRFI1*, *ESR1*, *ESR2*, *ETNK1*, *ETS1*, *ETV1*, *ETV4*, *ETV5*, *ETV6*, *EWSR1*, *EXO1*, *EXT1*, *EXT2*, *EZH1*, *EZH2*, *FAM175A*, *FAM46C*, *FAN1*, *FANCA*, *FANCB*, *FANCC*, *FANCD2*, *FANCE*, *FANCF*, *FANCG*, *FANCI*, *FANCL*, *FANCM*, *FAS*, *FAT1*, *FBXW7*, *FES*, *FGF10*, *FGF14*, *FGF19*, *FGF2*, *FGF23*, *FGF3*, *FGF4*, *FGF5*, *FGF6*, *FGFBP1*, *FGFR1*, *FGFR2*, *FGFR3*, *FGFR4*, *FH*, *FKBP1A*, *FLCN*, *FLI1*, *FLT1*, *FLT4*, *FOXA1*, *FOXA2*, *FOXE1*, *FOXL2*, *FOXO1*, *FOXO3*, *FOXP1*, *FOXQ1*, *FRK*, *FRS2*, *FUBP1*, *FUS*, *FYN*, *G6PD*, *GABRA6*, *GALNT12*, *GATA1*, *GATA2*, *GATA3*, *GATA4*, *GATA6*, *GLDN*, *GLI1*, *GLI2*, *GNA11*, *GNA13*, *GNAQ*, *GNAS*, *GPC3*, *GPER1*, *GPR124*, *GREM1*, *GRIN2A*, *GRM3*, *GSK3A*, *H3F3A*, *HCK*, *HGF*, *HIF1A*, *HIST1H3B*, *HLA-A*, *HLA-B*, *HLA-C*, *HLA-DPA1*, *HLA-DPB1*, *HLA-DQA1*, *HLA-DQB1*, *HLA-DRA*, *HLA-DRB1*, *HLF*, *HMGA2*, *HMGN1*, *HMOX2*, *HNF1A*, *HNF1B*, *HOXB13*, *HOXD8*, *HRAS*, *HSD3B1*, *HSP90AA1*, *HSP90AB1*, *ID3*, *IDH1*, *IDH2*, *IFNGR1*, *IFNGR2*, *IGF1R*, *IGF2*, *IGF2R*, *IKBKB*, *IKBKE*, *IKZF1*, *IKZF3*, *IL1B*, *IL1RN*, *IL2*, *IL21R*, *IL6*, *IL6ST*, *IL7R*, *ING4*, *INPP4B*, *INPPL1*, *IRF1*, *IRS2*, *ITK*, *JAK1*, *JAK2*, *JAK3*, *JUN*, *KAT6A*, *KDM5A*, *KDM5C*, *KDM6A*, *KDR*, *KEAP1*, *KIAA1549*, *KIT*, *KLF2*, *KLF4*, *KLHDC8B*, *KLHL6*, *KMT2A*, *KMT2B*, *KMT2C*, *KMT2D*, *KRAS*, *LATS1*, *LATS2*, *LCK*, *LIG4*, *LIMK2*, *LMO1*, *LRP1B*, *LRRK2*, *LTK*, *LYN*, *LZTR1*, *MAD2L2*, *MAFB*, *MAGEA1*, *MAGI1*, *MAGI2*, *MAML1*, *MAP2K1*, *MAP2K2*, *MAP2K3*, *MAP2K4*, *MAP2K5*, *MAP2K6*, *MAP2K7*, *MAP3K1*, *MAP3K14*, *MAP3K3*, *MAP3K4*, *MAP3K6*, *MAPK1*, *MAPK11*, *MAPK12*, *MAPK3*, *MAPK8IP1*, *MAX*, *MBD1*, *MC1R*, *MCL1*, *MDC1*, *MDM2*, *MDM4*, *MECOM*, *MED12*, *MEF2B*, *MEN1*, *MET*, *MGA*, *MGMT*, *MITF*, *MLH1*, *MLH3*, *MLLT10*, *MLLT3*, *MN1*, *MPL*, *MRE11A*, *MS4A1*, *MSH2*, *MSH3*, *MSH4*, *MSH5*, *MSH6*, *MSR1*, *MST1R*, *MTHFR*, *MTOR*, *MTRR*, *MUC1*, *MUC16*, *MUTYH*, *MXI1*, *MYB*, *MYC*, *MYCL*, *MYCN*, *MYD88*, *MYH11*, *MYH9*, *NBN*, *NCOA1*, *NCOA3*, *NCOR1*, *NF1*, *NF2*, *NFE2L2*, *NFKB1*, *NFKB2*, *NFKBIA*, *NFKBIE*, *NIN*, *NLRC5*, *NOP10*, *NOTCH1*, *NOTCH2*, *NOTCH3*, *NOTCH4*, *NPM1*, *NQO1*, *NR1I3*, *NRAS*, *NRG2*, *NSD1*, *NT5C2*, *NTHL1*, *NTRK1*, *NTRK2*, *NTRK3*, *NUMA1*, *NUP98*, *PAK3*, *PALB2*, *PALLD*, *PARK2*, *PARP1*, *PARP2*, *PARP4*, *PAX3*, *PAX5*, *PAX7*, *PBK*, *PBRM1*, *PBX1*, *PDCD1*, *PDCD1LG2*, *PDF*, *PDGFA*, *PDGFB*, *PDGFC*, *PDGFD*, *PDGFRA*, *PDGFRB*, *PDK1*, *PGR*, *PHF6*, *PHOX2B*, *PIAS4*, *PIGA*, *PIK3C2A*, *PIK3C2B*, *PIK3C2G*, *PIK3CA*, *PIK3CB*, *PIK3CD*, *PIK3CG*, *PIK3R1*, *PIK3R2*, *PIK3R3*, *PIM1*, *PKHD1*, *PLCG1*, *PLCG2*, *PML*, *PMS1*, *PMS2*, *POLD1*, *POLE*, *POLH*, *POLQ*, *POT1*, *PPM1D*, *PRDM1*, *PRDM16*, *PREX2*, *PRF1*, *PRKAR1A*, *PRKCA*, *PRKD1*, *PRKDC*, *PROM2*, *PRSS1*, *PRX*, *PSIP1*, *PSMB1*, *PSMB10*, *PSMB2*, *PSMB5*, *PSMB8*, *PSMB9*, *PSMC3IP*, *PSPH*, *PTCH1*, *PTCH2*, *PTEN*, *PTGS2*, *PTK2*, *PTK7*, *PTPN11*, *PTPRC*, *PTPRD*, *PTPRT*, *RAC1*, *RAC2*, *RAD21*, *RAD50*, *RAD51*, *RAD51B*, *RAD51C*, *RAD51D*, *RAD54B*, *RAD54L*, *RAF1*, *RALGDS*, *RARA*, *RARB*, *RARG*, *RASA1*, *RASAL1*, *RB1*, *RBM10*, *RECQL4*, *REL*, *RET*, *RFC2*, *RFX5*, *RHBDF2*, *RHEB*, *RHOA*, *RICTOR*, *RINT1*, *RIPK1*, *RIT1*, *RNASEL*, *RNF2*, *RNF43*, *ROS1*, *RPL22*, *RPS20*, *RPS6KB1*, *RPTOR*, *RSF1*, *RUNX1*, *RYR1*, *SACS*, *SAMHD1*, *SAV1*, *SBDS*, *SCG5*, *SDHA*, *SDHAF2*, *SDHB*, *SDHC*, *SDHD*, *SEC23B*, *SEMA4A*, *SETBP1*, *SETD2*, *SETDB1*, *SF3B1*, *SGK1*, *SH2B1*, *SH2B3*, *SH2D1A*, *SHFM1*, *SHH*, *SIK2*, *SIN3A*, *SIRT1*, *SKP2*, *SLC26A3*, *SLIT2*, *SLX4*, *SMAD3*, *SMAD4*, *SMARCA4*, *SMARCB1*, *SMARCE1*, *SMC1A*, *SMC3*, *SMO*, *SOCS1*, *SOX11*, *SOX2*, *SOX9*, *SPEN*, *SPINK1*, *SPOP*, *SPRED1*, *SPTA1*, *SRC*, *SRD5A2*, *SRGAP1*, *SRP72*, *SRSF2*, *SSTR1*, *SSTR2*, *SSTR3*, *SSTR5*, *SSX1*, *STAG1*, *STAG2*, *STAT1*, *STAT3*, *STAT5A*, *STAT5B*, *STK11*, *SUFU*, *SUZ12*, *SYK*, *TAF1*, *TAF15*, *TAP1*, *TAP2*, *TBK1*, *TBL1XR1*, *TBX3*, *TCF3*, *TCF7L2*, *TCL1A*, *TEK*, *TERC*, *TERF2IP*, *TERT*, *TET1*, *TET2*, *TFE3*, *TGFBR2*, *TLR4*, *TLX1*, *TMEM127*, *TNF*, *TNFAIP3*, *TNFRSF11A*, *TNFRSF13B*, *TNFRSF14*, *TNFRSF1A*, *TNFRSF1B*, *TNFRSF25*, *TNFRSF8*, *TNFSF11*, *TNK2*, *TOP1*, *TOP2A*, *TP53*, *TP53BP1*, *TPX2*, *TRAF2*, *TRAF3*, *TRAF5*, *TRAF6*, *TRAF7*, *TRRAP*, *TSC1*, *TSC2*, *TSHR*, *TUBA4A*, *TUBB*, *TYMS*, *U2AF1*, *UBE2T*, *UBR5*, *UGT2B15*, *UGT2B7*, *UIMC1*, *UNG*, *USP34*, *USP9X*, *VEGFA*, *VEGFB*, *VHL*, *VKORC1*, *WAS*, *WASF3*, *WHSC1*, *WISP3*, *WRN*, *WT1*, *XIAP*, *XPA*, *XPC*, *XPO1*, *XRCC1*, *XRCC2*, *XRCC3*, *XRCC5*, *XRCC6*, *YAP1*, *ZFHX3*, *ZHX3*, *ZNF217*, *ZNRF3*, *ZRSR2* (somatic tumor panel version 4)

Translocations

Genomic regions known to be frequently involved in translocation events are additionally enriched using the Agilent in solution technology. The alignment is bioinformatically checked for potential translocations apparent by discordant read pairs and split reads. Regions of interest are visually reviewed and possible translocations are manually annotated.

Translocations potentially affecting the following genes are being assessed:

ALK, *BCL2*, *BCR*, *BRAF*, *BRD4*, *EGFR*, *ERG*, *ETV4*, *ETV6*, *EWSR1*, *FGFR1*, *FGFR2*, *FGFR3*, *FUS*, *MYB*, *MYC*, *NOTCH2*, *NTRK1*, *PAX3*, *PDGFB*, *RARA*, *RET*, *ROS1*, *SSX1TFE3*, *SUZ12*, *TAF15*, *TCF3*, *TMPRSS2*

Methods

DNA isolation: DNA from tumor tissue was isolated after macrodissection at the Praxis für Humangenetik, Tübingen.

NGS-laboratory: The coding areas and the adjacent intronic junctions of DNA from tumor and normal tissue were enriched using Agilent in-solution technology and subsequently analyzed using high-throughput sequencing on the Illumina HiSeq/NovaSeq system.

Computational analysis: Illumina bcl2fastq2 was used to demultiplex sequencing reads. Adapter removal was performed with Skewer. The trimmed reads were mapped to the human reference genome (hg19) using the Burrows Wheeler Aligner. Reads mapping to more than one location with identical mapping score were discarded. Read duplicates that likely result from PCR amplification were removed. The remaining high quality sequences were used to determine sequence variants (single nucleotide changes and small insertions/deletions). The variants were annotated based on several internal as well as external databases.

Genetic data evaluation: Only variants (SNVs/small indels) with a novel allele frequency (NAF) of ≥ 5% in the tumor sample within the coding regions and their adjacent intronic regions (-/+ 8 base pairs) were evaluated. A list of all the variants with an allele frequency of 5% considered in the genetic data evaluation can be requested at any time. The clinical interpretation of variants is based on different external and internal databases and on information from scientific literature. The sensitivity of the test is depending on the tumor load, the sample quality and sequencing depth. A coverage of 120 reads per base achieves a theoretical sensitivity of 99% for the detection of variants with a ≥ 10% NAF. In this case, 95.1% of the targeted regions were covered by a minimum of 120 high-quality sequencing reads per base. Variants are named according to the HGVS recommendations without any information regarding the cis or trans configuration.

Mutational load: The mutational load is defined as the number of somatic SNV-, InDel- and essential splice-site variants (NAF >=0.1) per megabase of coding DNA. Mutational load on exom level is extrapolated, taking the results of panel data analysis as a basis. Truncating variants in tumor suppressor genes as well as somatic variants with an inhouse frequency of ≥ 1% are not accounted. The mutational load is classified low (0-3.3 mut/Mbp), intermediate (3.3-23.1 mut/Mbp) or high (≥ 23.1 mut/Mbp) (Chalmers et al., 2017, PMID: 28420421; Johnson et al., 2016, PMID: 27671167).

Microsatellite instability (MSI): A polymerase chain reaction (PCR) was performed for five marker loci, each spanning a mononucleotide microsatellite stretch (BAT25, BAT26, NR21, NR22, NR27) using DNA from germline and tumor tissue (Hegde et al., 2014, PMID: 24310308; Pagin et al., 2013, PMID: 23652311; Goel et al., 2010, PMID: 20195377). This was followed by separation and size comparison of the PCR fragments by capillary electrophoresis. Instability of a single marker is designated MSI-low, instability of ≥2 marker is designated MSI-high. Tumor samples for which no instability is detected are referred to as MSS (microsatellite stable). In case of insufficient data, MSI status can additionally be predicted from sequencing data (step-wise difference (DIF); threshold 0,4; Kautto et al., 2017, PMID: 27980218). Please be aware that bioinformatics MSI prediction cannot replace a validated diagnostic test for MSI.

The sample fulfilled our quality criteria upon arrival and during/after each processing step in the laboratory.

The procedure described above was developed and validated in-house (Laboratory developed test; LDT). A minimal tumor content of 20% was taken as a basis.

Communication, dissemination and usage of this report for scientific purposes is only permitted in accordance to applicable law (GenDG).

SUPPLEMENTARY INFORMATION – MUTATIONAL LOAD

The figure shows the approximated mutational load of the previously described tumor sample (red bar) in relation to the mutational load published for different tumor entities (Lawrence et al., 2013, PMID: 23770567). The mutational load on exome level is extrapolated, taking the results of panel data analysis as a basis. The mutational load is classified low (0-3.3 mut/Mbp), intermediate (3.3-23.1 mut/Mbp) or high (≥23.1 mut/Mbp) according to Johnson et al. (2016, PMID: 27671167). A high mutational load has been associated with a superior response to immune therapy approaches in different tumor entities (Johnson et al., 2016, PMID: 27671167; Rizvi et al., 2015, PMID: 25765070; Snyder et al., 2014, PMID: 25409260; Le et al., 2015, PMID: 26028255; Bouffet et al., 2016, PMID: 27001570).

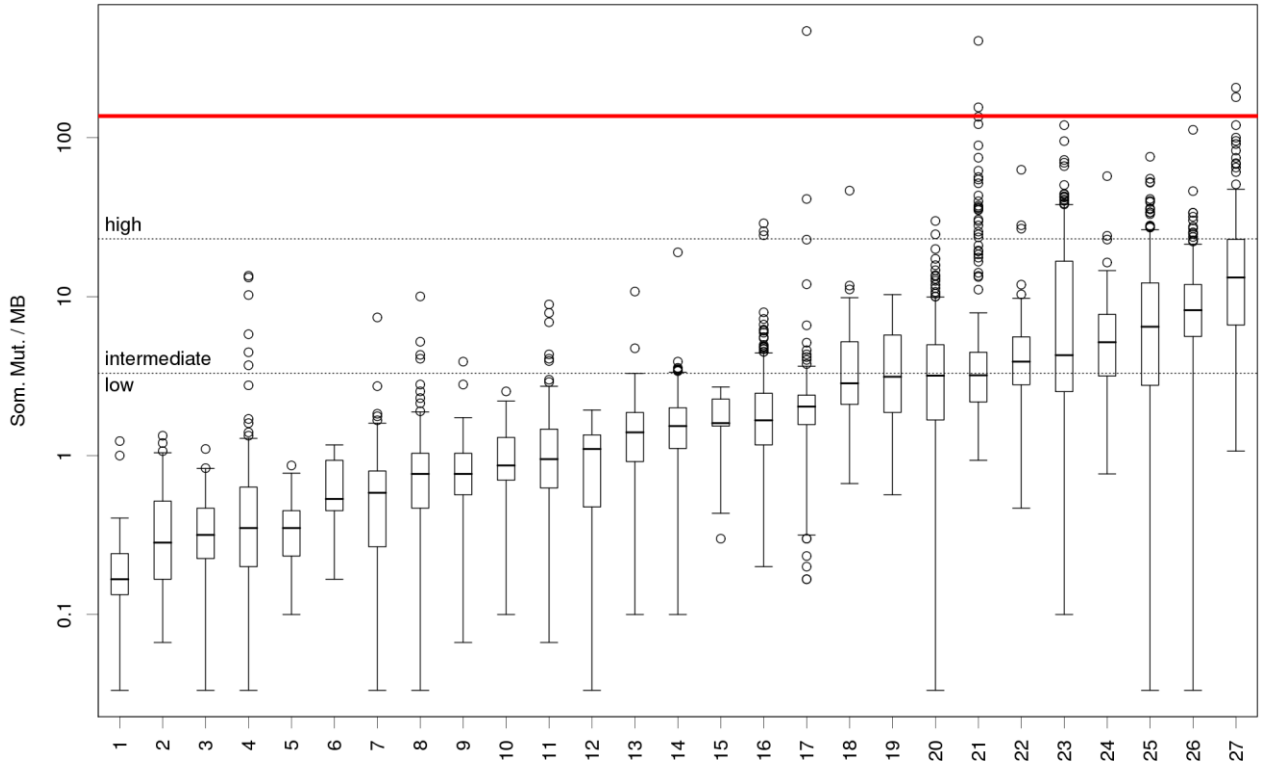

Distribution of mutational load in 27 tumor entities

The distribution of mutational load (somatic variants per megabase of coding DNA) is shown for 27 different tumor entities (n=3083). Boxplots show the range containing 50% of all values (interquartile range, IQR, between percentile 75 and 25) as boxes, medians as solid horizontal lines. Outliers (circles) are shown for values deviating by more than 1.5 times the IQR (indicated by vertical lines). The mutational load of 2.7 mut/Mbp determined for the current case is shown for comparison (solid red line). Y-axis is log scaled. The classification into low (<3.3 mut/Mbp), intermediate (3.3-23.1 mut/Mbp), and high (>23.1 mut/Mbp) mutational loads as described by Johnson et al. (2016, PMID: 27671167) is indicated with dashed lines.

Entities are: (1) Rhabdoid tumor, (2) Ewing Sarcoma, (3) Thyroid cancer, (4) Acute myeloid leukemia, (5) Medulloblastoma, (6) Carcinoid, (7) Neuroblastoma, (8) Prostate cancer, (9) Chronic lymphocytic leukemia, (10) Low-grade glioma, (11) Breast cancer, (12) Pancreatic cancer, (13) Multiple myeloma, (14) Kidney clear cell, (15) Kidney papillary cell, (16) Ovarian cancer, (17) Glioblastoma multiforme, (18) Cervical cancer, (19) Diffuse large B-cell lymphoma, (20) Head and neck carcinoma, **(21) Colorectal cancer**, (22) Esophageal adenocarcinoma, (23) Gastric cancer, (24) Bladder carcinoma, (25) Lung adenocarcinoma, (26) Lung squamous cell carcinoma, (27) Melanoma (Figure modified referring to Lawrence et al., 2013, PMID: 23770567).

SUPPLEMENTARY INFORMATION – ADDITIONAL SOMATIC VARIANTS

The following somatic variants were classified as having no current therapeutic relevance.

Gene	Functional category	Variant	Transcript-ID	NAF
AR	missense	p.Ala412Val	NM_000044.3	0.44
DNMT3A	missense	p.Arg181His	NM_022552.4	0.23
EPHA5	synonymous	p.=	NM_004439.6	0.30
FGFR1	missense	p.Asp132Val	NM_015850.3	0.26
NTRK3	missense	p.Leu238Ile	NM_002530.3	0.39
PRKACA	splice_region	p.?	NM_002730.3	0.26
PRKD1	missense	p.Asn195Ser	NM_002742.2	0.27
PRKD1	splice_region	p.?	NM_002742.2	0.32
REL	synonymous	p.=	NM_002908.3	0.21
RUNX1T1	missense	p.Arg367Gln	NM_004349.3	0.39
RYR1	missense	p.Arg1583His	NM_000540.2	0.32
SMAD4	missense	p.Cys363Tyr	NM_005359.5	0.32
SMAD4	missense	p.Trp524Gly	NM_005359.5	0.32
SPTA1	missense	p.Arg1694Cys	NM_003126.2	0.14
SRSF2	missense	p.Pro46Gln	NM_003016.4	0.26
TAL1	synonymous	p.=	NM_003189.5	0.15

NAF: *Novel allele frequency*, the frequency with which the mutated allele was detected in the sequencing data (1 is 100%). The observed frequencies are influenced by the tumor content and do not correlate directly with the variant frequency in the tumor.

CeGaT GmbH | Paul-Ehrlich-Str. 23 | D-72076 Tübingen | Germany
Tel: + 49 7071 565 44 55 | Fax: + 49 7071 565 44 56 | info@cegat.de | www.cegat.de
Court District Stuttgart - HRB 729958 | VAT No: DE265504070
VR Bank Tübingen eG | IBAN: DE20 6406 1854 0021 2890 00 | SWIFT / BIC: GENODES1STW
Managing Directors: Dr. Dr. Saskia Biskup, Dr. Dirk Biskup

SUPPLEMENTARY INFORMATION – POSSIBLE THERAPEUTIC STRATEGIES

Target specificities of the following drugs are mainly based on the information of www.selleckechem.com or http://adisinsight.springer.com.

The approval drug status or clinical trial status (which include withdrawn, terminated, finished and ongoing studies) are periodically updated and based on the information given by the FDA, EMA, www.cinicaltrials.gov and http://adisinsight.springer.com homepages.

High mutational load and MSI, germline mutation *MSH6*, c.3132C>A; p.Tyr1044*, NM_000179.2

Relevant immune checkpoint inhibitors:

Drug name	Rationale	status
Nivolumab (Opdivo)	Anti-PD1 monoclonal antibody	EMA approved: Melanoma, Non-small cell lung carcinoma (NSCLC), Renal cell carcinoma, Hodkin lymphoma (HL), Head and neck squamous cell carcinoma (HNSCC) FDA approved: Hodkin lymphoma (HL), Melanoma, Non-small cell lung carcinoma (NSCLC), Renal cell carcinoma, Head and neck squamous cell carcinoma (HNSCC), Urothelial carcinoma
Atezolizumab (Tecentriq)	Anti-PD-L1 monoclonal antibody	FDA approved: Urothelial carcinoma, Non-small cell lung carcinoma (NSCLC)
Pembrolizumab (Keytruda)	Anti-PD-1 monoclonal antibody	FDA approved: Melanoma, Non-small cell lung carcinoma (NSCLC), Head and neck squamous cell carcinoma (HNSCC), Hodgkin lymphoma (HL) EMA approved: Melanoma, Non-small cell lung carcinoma (NSCLC)
Durvalumab (Imfinzi)	Anti-PD-L1 monoclonal antibody	FDA approved: Urothelial carcinoma Phase 2: Solid tumor Phase 3: Non-small cell lung carcinoma (NSCLC), Head and neck squamous cell carcinoma (HNSCC), Bladder carcinoma, Breast carcinoma
Avelumab (Bavencio)	Anti-PD-L1 monoclonal antibody	FDA approved: Merkel-cell carcinoma Phase 1: Solid tumor Phase 3: Gastric carcinoma, Non-small cell lung carcinoma (NSCLC), Renal cell carcinoma, Ovarian carcinoma, Urothelial carcinoma
Pidilizumab	Anti-PD-L1 monoclonal antibody	Phase 2: Glioblastoma, Melanoma, Renal cell carcinoma, Acute myelocytic leukemia (AML), Multiple myeloma (MM), Colorectal carcinoma, Follicular lymphoma (FL), Diffuse large B-cell lymphoma (DLBCL)
AMP-224	Anti-PD-1 fusion protein	Phase 1: Solid tumor
BMS-936559	Anti-PD-L1 monoclonal antibody	Phase 1: Solid tumor

NRAS, c.35G>A; p.Gly12Asp, NM_002524.4:

Relevant therapeutics for biomarker *NRAS*:

Drugname	Rationale	Status
Trametinib (Mekinist)	MEK1,2 inhibitor	Phase 2: Colorectal carcinoma FDA and EMA approved: Melanoma
Cobimetinib (Cotellic)	MEK1 inhibitor	Phase 1: Solid Tumor FDA Approved: Melanoma
Selumetinib	MEK1,2 inhibitor	Phase 2: Colorectal carcinoma Phase 3: Melanoma, Non-small cell lung carcinoma (NSCLC), Uveal melanoma, Thyroid carcinoma
Binimetinib	MEK1,2 inhibitor	Phase 1: Colorectal carcinoma Phase 3: Melanoma, Ovarian carcinoma
Refametinib	MEK1 inhibitor	Phase 2: Colorectal carcinoma Phase 2: Gallbladder carcinoma, Hepatocellular carcinoma, Pancreatic carcinoma, Non-small cell lung carcinoma (NSCLC), Breast carcinoma, Cholangiocarcinoma
PD0325901	MEK1,2 inhibitor	Phase 2: Colorectal carcinoma Phase 2: Pancreatic carcinoma, Melanoma, Non-small cell lung carcinoma (NSCLC), Breast carcinoma, Neurofibromatosis type 1
Pimasertib	MEK1,2 inhibitor	Phase 2: Colorectal carcinoma Phase 2: Melanoma, Pancreatic ductal adenocarcinoma, Hematologic malignancies
Defactinib	Second-generation FAK and Pyk2 inhibitor	Phase 1: Solid Tumor Phase 2: Mesothelioma

TP53, c.672+1G>T; p.?, NM_000546.5:

Relevant therapeutics for biomarker *TP53*

drug	targets	status
Alisertib	Aurora A Small molecule kinase inhibitor	Clinical Trials
ALT-801	p53-targeted T-Cell receptor-IL2 fusion	Clinical Trials
MK-1775	Wee1 tyrosine kinase inhibitor	Clinical Trials
SGT-53	TP53 gene therapy delivered via transferrin-targeted nanoparticles	Clinical Trials
ENMD-2076	Aurora A Small molecule kinase inhibitor	Clinical Trials
APR-246	Reactivates mutant p53	Clinical Trials
AMG 900	Aurora A, B, C Small molecule kinase inhibitor	Clinical Trials
TAS-119	Selective Aurora A kinase inhibitor	Clinical Trials
Kevetrin	Interferes with p53-MDM2 interaction, re-activates wild-type p53	Clinical Trials
COTI-1	P53 gene modulator	Clinical Trials